Supporting Information
for
Nonlinear Scaling of Surface Water Diffusion with Bulk Water Viscosity of Crowded Solutions

John M. Franck, John A. Scott, and Songi Han*
Department of Chemistry and Biochemistry, University of California, Santa Barbara, California 93106
Received February 6, 2013; E-mail: songi@chem.ucsb.edu

All compounds were acquired from commercial vendors and used without further purification. DPPC (1,2-dipalmitoyl-*sn*-glycero-3-phosphocholine) and 16:0 Tempo PC (1,2-dipalmitoyl-*sn*-glycero-3-phospho(tempo)choline) were acquired from Avanti Polar Lipids (Alabaster, AL). Ficoll 70 and sucrose were acquired from Sigma-Aldrich (St. Louis, MO). PBS buffer (phosphate buffered saline), was prepared from 150 mM NaCl and 50 mM phosphate and titrated to pH 7.6. The NaCl, sodium phosphate (monobasic and dibasic), as well as the chloroform and methanol solvents used for dissolution of the lipids were acquired from Fisher Scientific (Pittsburg, PA).

Dissolution of lipids A solution of DPPC in 90%:10% (v/v) choloform:methanol was dried in a culture tube under flow of dry N_2 gas, rotating during the final stages of drying to ensure a thin lipid film of relatively uniform thickness. The films were dried overnight under vacuum. For samples used in determining ODNP enhancements, 3 mol % 16:0 Tempo PC was mixed into the chloroform and methanol solution before drying, ultimately yielding a spin label concentration of 960 µM. An appropriate quantity ($\sim$ 400 µL) of PBS buffer (to enforce a constant pH) was added to generate a 32 mM solution of lipids. The resulting solution was vortexed for 1 hr at 60°C.

Preparation of LUV Half of the dissolved lipid solution was removed and extruded 10 times at 60°C with the Mini-Extruder from Avanti polar lipids (part #610000, operated with 250 µL Hamilton syringes) through a filter with 200 nm pores (polycarbonate membrane 0.2 µm 19 mm, Avanti part #610006). The resulting sample constituted the LUV (large unilamellar vesicles) sample.

Preparation of MLV The other half of the dissolved lipid was subjected to 5 "freeze-thawing" cycles of the main lipid phase transition. These consisted of 10 min of resting at 60°C, a short period of vortexing, and 10 min of resting at 0°C.[1,2] This latter sample constituted the MLV (multilamellar vesicle) sample.

Addition of viscogens Samples of both Ficoll LUV and MLV samples were prepared with two different crowding agents added, namely macromolecular Ficoll and the small molecule sucrose. In both cases, enough of the crowding agent was added to increase the viscosity of the solution by 10 fold compared to bulk water, *i.e.* from 8.9 cP to 89 cP (viscosity of water is 0.89 cP=0.89 mPa · s at 25°C). To avoid errors during vesicle extrusion or during the measurement of volumes with standard pipettes, higher viscosities were not attempted.

Ficoll samples: A solution with 21 % (w/v) Ficoll 70 has a viscosity slightly greater than 10 times that of water;[1] therefore, a solution of 45% (w/v) Ficoll 70 was prepared and mixed into the previously prepared vesicle solution in a 50% (v/v) ratio shortly before the measurements.

Sucrose samples: A solution with 45.7% sucrose has a viscosity 10 times that of water.[3] The 91.4% sucrose solution that would be needed to mix sucrose into the solution after vesicle preparation would be supersaturated, so identical, separate MLV and LUV samples containing sucrose were dissolved and prepared in a solution of 45.7% sucrose in PBS, which was mixed with 50% (v/v) of 45.7% sucrose in PBS shortly before the measurements.

ODNP A volume of 3.0 µL-3.5 µL of the mixed sample was added to a 0.6 mm i.d. 0.84 mm o.d. quartz capillary tube. The NMR signal of this sample was detected in the presence of varying amounts of ESR-resonant microwave irradiation in order to detect the ODNP NMR signal enhancement, and the NMR relaxation times were also determined, as subsequently discussed. From this set of measurements, we calculated the cross-relaxivity, k_σ, and the self-relaxivity, k_ρ, of water protons in the presence of the spin label. (Here, we use the term "relaxivity" to indicate concentration-scaled relaxation rates, which therefore have units of $s^{-1}M^{-1}$.) These two values were compared in order to determine the correlation time, τ_c, as also detailed in this section.

A home-built NMR probe was inserted into a 3 mm o.d. ESR tube located inside a standard TE011 (cylindrical) commercial ESR cavity (ER 4119HS-LC from Bruker, Billerica, MA). The probe comprised a simple copper wire construction with teflon supports that were designed to hold the 0.84 mm o.d. capillary tube and fit inside the 3 mm tube. The entire setup is positioned inside the gap of a commercial ESR magnet (Bruker EMXplus), and air was flowed through the 3 mm ESR tube at a rate of $\sim$9 L/min to help stabilize the sample near ambient temperature (24°C).

The probe was connected to a tuning circuit and a Bruker Avance NMR console.[4] The NMR signal (Fig. 1(a)), arises from the protons of water and was measured with a standard 90° rf pulse followed by a repetition delay of at least $5 \times T_{1,max}$, where $T_{1,max}$ is the maximum longitudinal relaxation time of the protons in water (accounting for slight heating effects, *etc.*[5]).

The microwave frequency was matched to the resonance of the ESR cavity, the magnetic field was set so that the microwave frequency was resonant with the central ESR transition of the (TEMPO-based) spin label, and the NMR signal level was measured for a series of microwave powers, p, ranging from 0 to 4.5 W. (Microwave power was supplied by a home-built microwave amplifier with a design similar to previously published designs.[4]) This allows us to calculate the ODNP signal enhancements, $E(p)$, as shown in Fig. 1(b). The first step in determining the correlation time, τ_c, is to isolate the value of k_σ from these enhancement ($E(p)$) values.

The NMR signal enhancements, $E(p)$, are determined by a bal-

[1] GE Healthcare Data File 18-1158-27 AB

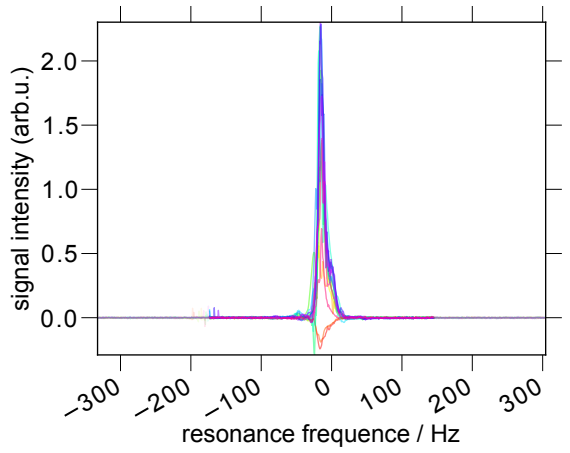

(a) NMR spectra

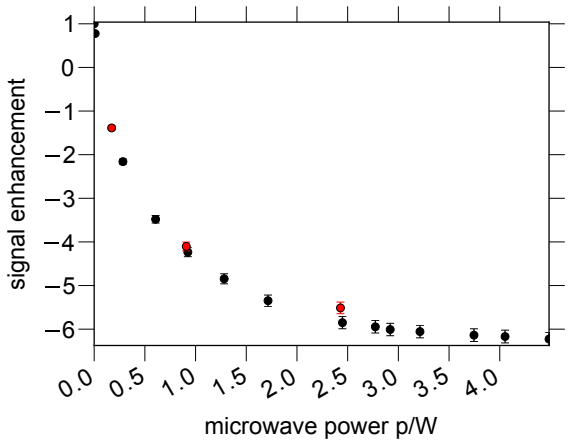

(b) ODNP enhancements

Figure 1. water NMR signals at various powers (the various colors in Fig. 1(a)), are integrated, then divided by the integral at zero power (*i.e.* the thermal equilibrium signal) to yield a series of ODNP signal enhancements, Fig. 1(b); the enhancements plotted in black were taken at sequentially increasing microwave powers, then those in red were taken at sequentially decreasing microwave powers.

ance between the rate of relaxation to thermal equilibrium and the rate of hyperpolarization[5]

$$1 - E(p) = \overbrace{T_1(p)}^{1/\text{rate of thermal relaxation}} \overbrace{k_\sigma s(p) C_{SL} \left| \frac{\omega_e}{\omega_H} \right|}^{\text{rate of hyperpolarization}}; \qquad (1)$$

where $T_1(p)$ is the NMR longitudinal relaxation time – *i.e.* the time constant for relaxation of the NMR signal to thermal equilibrium; as noted above, k_σ is the cross-relaxivity between the electron and proton spins – *i.e.* the ratio of ODNP-driven rate of cross-relaxation between the electron and proton spins to the concentration; $s(p)$ is the saturation factor (the net electron spin saturation across all three hyperfine transitions of the nitroxide) for a range of microwave powers, p; C_{SL} is the concentration of the spin label; and ω_H and ω_e are the proton and electron Larmor frequencies, respectively.

By acquiring the rate of relaxation to thermal equilibrium, $T_1^{-1}(p)$, at several different microwave powers, p, (Figs. 2(a) and 2(b)) we can then accurately retrieve a value for the cross-relaxivity, k_σ. Specifically, the enhancements and relaxation times yield the values of $k_\sigma s(p)$, as shown in Fig. 2(c), when

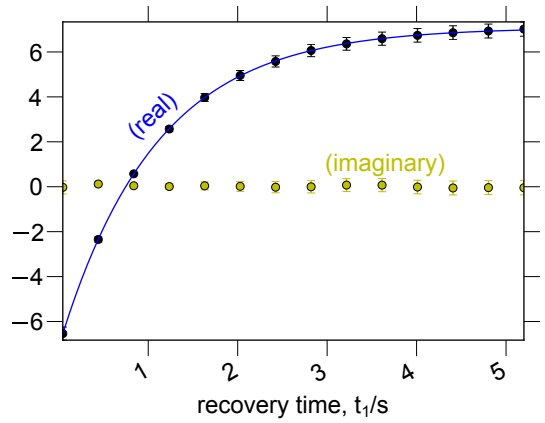

(a) Inversion-recovery results

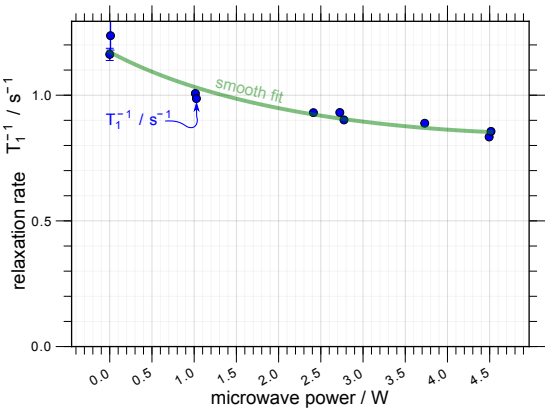

(b) $T_1(p)$ vs. microwave power, p

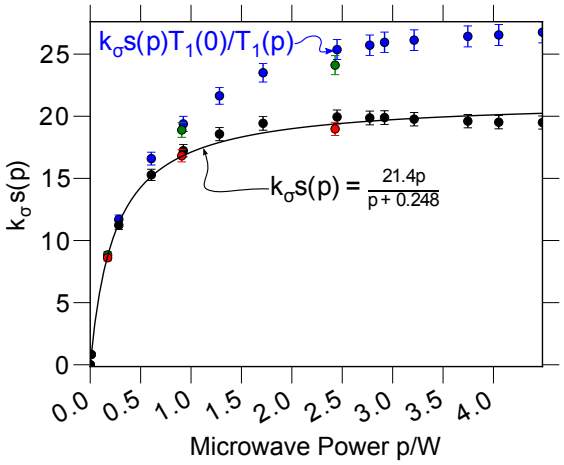

(c) $k_\sigma s_{max}$ fitting procedure

Figure 2. Illustrates how the enhancements are converted from enhancement values, $E(p)$, to $k_\sigma s_{max}$. A series of inversion recovery experiments (top) were fit to yield NMR longitudinal relaxation (*i.e.* T_1) times at several different powers (middle plot); subsequently, the values of these points were fit to a smooth curve (green line, middle plot), as described in the text. The smooth curve provides $T_1(p)$ as a function of power. Finally, (bottom, red/black) the values of the enhancements are divided by the value of $T_1(p)$ and fit to an asymptotic curve to yield $k_\sigma s_{max}$. Here, we also show that not accounting for the variation of T_1 with microwave power (as a result of mild sample heating) does yields a significantly different results. Specifically, the second curve (in blue/green) displays the the values that result when the enhancements are all divided by $T_1(p = 0)$.

inserted into the equation

$$k_\sigma s(p) = \frac{1-E(p)}{C_{SL} T_1(p)} \left| \frac{\omega_H}{\omega_e} \right| \tag{2}$$

which is rearranged from Eq. (1), and where the ratio of the Larmor frequencies, $|\omega_H/\omega_e|$ remains stable at $\omega_e/\omega_H \approx 1.5167‰$ (*i.e.* parts per thousand) for the experiments here. Next, these values are fit to the equation

$$k_\sigma s(p) = \frac{k_\sigma s_{max} p}{p_{1/2} + p}, \tag{3}$$

which includes the asymptotic dependence of $s(p)$ on microwave power,[6,7] where $p_{1/2}$ is the microwave power that achieves half saturation of the electron spin transition, and where the two fit parameters are $p_{1/2}$ and $k_\sigma s_{max}$.[5] By extrapolating to infinite microwave power, we find the limit of maximal saturation, *i.e.* $s(p) \to s_{max}$ so that $k_\sigma s(p) \to k_\sigma s_{max}$, allowing us to isolate k_σ. As explained elsewhere,[5,8,9] the determination of s_{max} is non-trivial, and its value can range anywhere between 1/3 and 1 for ^{14}N nitroxides; however for tethered spin probes $s_{max} \approx 1$ and therefore $k_\sigma \approx k_\sigma s_{max}$ provides a very good approximation.[6,8]

Having determined k_σ, we next determine k_ρ. The NMR relaxation time, $T_{1,0}$, of a sample without spin label is measured in the absence of microwaves (following a fitting procedure identical to Fig. 2(a)) and compared to the T_1 time of the spin labeled sample in the absence of microwaves to determine the proton self-relaxivity in the vicinity of the spin label, k_ρ. Specifically,

$$k_\rho = \frac{1}{C_{SL}} \left(\frac{1}{T_1} - \frac{1}{T_{1,0}} \right). \tag{4}$$

The ratio of the k_σ and k_ρ values gives the unitless coupling factor, $\xi = k_\sigma/k_\rho$, which can be interpolated onto the force-free hard-sphere (FFHS) model for translational dynamics,[5,6,10] to yield a value for the correlation time τ_c referenced in the main text. Each measurement of τ_c was repeated 2-4 times, and the standard deviation of the resulting measurements is presented as an error (*i.e.* as value $\pm$ error).

In the remainder of the Supporting Information, we present first how one efficiently determines the values of $T_1(p)$ for insertion into Eq. (2), and then very briefly derive how one can convert the pair of relaxivity measurements k_σ and k_ρ, which we have explained up to this point, into the more intuitive pair of measurements k_σ and k_{low}.

Interpolation of $T_1(p)$ Since the NMR longitudinal relaxation time varies as a function of microwave power, as a result of small amounts of microwave-induced heating, this method requires a means for measuring the microwave power dependence of the $T_1(p)$ time. However, inversion-recovery measurements of the NMR longitudinal relaxation (*i.e.* T_1) time can be relatively time consuming. Therefore, we require a means for measuring $T_1(p)$ at a limited number of microwave power levels (*i.e.* a limited set of p values) and interpolating between them.

For our purposes here, it is only important to note that we can generate a smooth and simple interpolation, as shown in Fig. 2(a) – *i.e.* the fact that the interpolated curve passes near the error bars of all the measured values shows that we have approximated reasonable $T_1(p)$ values at the intermediate microwave powers, p. However, to satisfy the reader's curiosity, we present the specific method by which we achieve this interpolation, and the motivation behind it.

The NMR longitudinal relaxation rate, $T_1^{-1}(p)$, at a specific microwave power, p, is given by

$$\frac{1}{T_1(p)} = C_{SL} k_\rho(p) + \frac{1}{T_{1,w} + p\Delta T_{1,w}} + k_{HH} C_{macro}, \tag{5}$$

where C_{SL} is the concentration of the spin label, $k_\rho(p)$ is the spin-label-induced self-relaxivity (units $\mathrm{s^{-1}M^{-1}}$), $T_{1,w}$ is the relaxation time of pure water in the absence of microwave power, $\Delta T_{1,w}$ is the variation of the relaxation time of pure water, which is roughly linear with power,[5] and $k_{HH}\, C_{macro}$ is the contribution (typically arising from proton-proton interactions) to the NMR relaxation rate from the macromolecule itself, which has a concentration of C_{macro}.

One can measure $\Delta T_{1,w}$ and $T_{1,w}$ for a given experimental setup. One can also determine the value of k_{HH} by measuring the relaxation time with the microwave power off (*i.e.* $p = 0$) and without any spin label added to the sample (*i.e.* $C_{SL} = 0$), then solving Eq. (5). The two concentrations, C_{SL} and C_{macro}, are known from the sample preparation. Therefore, for the limited set of (typically 5-8) microwave powers at which the $T_1(p)$ time is acquired, one can calculate $k_\rho^{-1}(p)$, *i.e.*

$$k_\rho^{-1}(p) = C_{SL} \left(\frac{1}{T_1(p)} - \frac{1}{T_{1,w} + p\Delta T_{1,w}} - k_{HH} C_{macro} \right)^{-1}. \tag{6}$$

We can surmise that $k_\rho^{-1}(p)$ is an approximately linear or second-order function of microwave power[2] over small enough microwave-induced temperature variations. Thus, by fitting the values of $k_\rho^{-1}(p)$ to a polynomial, then evaluating the polynomial at intermediate powers and reinserting the appropriate value of $k_\rho(p)$ into Eq. (5), one can retrieve an accurately interpolated value for $T_1(p)$ at any intermediate power. We have tested this procedure on a variety of different protein and lipid vesicle samples, and found that a polynomial of second order in power reasonably and routinely fits to $k_\rho^{-1}(p)$, yielding a subsequently reasonable interpolation similar to that shown in Fig. 2(a) (data not shown).

Derivation of k_{low} Ultimately both the relaxivities, k_σ and k_{low}, derive their usefulness to the study of hydration dynamics from the fact that they probe the value of the spectral density function for fluctuations in the proton-electron dipolar interaction, $J(\omega, \tau_c)$. Here, we explain how one can isolate the relaxivity k_{low}, which depends only on the value of the spectral density function at the NMR resonance frequency (*i.e.* $J(\omega_H, \tau_c)$ where $\omega_H \sim 2\pi \times 15$ MHz for these experiments) and therefore can serve as an important tool for probing hydration dynamics on a slower timescale. While the determination of k_{low} does not serve a pivotal role in the results that we have determined here, we begin to introduce this concept here since we believe it will play an important role in future work.

We approximate $\omega_e \pm \omega_H \approx \omega_e$, where the ω give the resonance frequencies of the electron and proton, respectively. This approximation is nearly exact, since $\omega_e/\omega_H = 1.5167‰$ for nitroxide spin labels in aqueous solution. Next, we calculate the relaxivities and the coupling factor in terms of the spectral density function, $J(\omega, \tau_c)$, of the dipole-dipole Hamiltonian[7,11]

$$\begin{aligned} k_\sigma(B_0, \tau_c) &= 6J((\gamma_e - \gamma_H)B_0, \tau_c) - J((\gamma_e + \gamma_H)B_0, \tau_c) \\ &\approx 5J(\gamma_e B_0, \tau_c) \end{aligned} \tag{7}$$

$$\begin{aligned} k_\rho(B_0, \tau_c) &= 6J((\gamma_e - \gamma_H)B_0, \tau_c) + 3J(\gamma_H B_0, \tau_c) \\ &\quad + J((\gamma_e + \gamma_H)B_0, \tau_c) \\ &\approx 7J(\gamma_e B_0, \tau_c) + 3J(\gamma_H B_0, \tau_c). \end{aligned} \tag{8}$$

where γ_e and γ_H give the gyromagnetic ratios of the electron and

[2] In the extreme narrowing limit, $k_\rho^{-1}(p)$ is proportional to the correlation time. This leads us to expect that in more general cases, sufficiently small changes to microwave power will lead k_ρ^{-1} to approach a linear response regime.

proton, and B_0 gives the magnetic field, such that $\omega_e = \gamma_e B_0$ and $\omega_H = \gamma_H B_0$.[3] For simplicity, here the spectral density function that we have denoted is scaled by concentration and so has units $\mathrm{s}^{-1}\mathrm{M}^{-1}$. Though we show a single correlation time, τ_c, the math and approximations are equally valid for a system described by multiple timescales of dynamics, as long as the ODNP arises from a dipolar mechanism. Eqs. (7) and (8) in turn yield an expression for the ODNP coupling factor, ξ

$$\begin{aligned}\xi(B_0,\tau_c) &= \frac{k_\sigma}{k_\rho} \qquad (9)\\ &= \Big(6J((\gamma_e-\gamma_H)B_0,\tau_c) - J((\gamma_e+\gamma_H)B_0,\tau_c)\Big)\\ &\quad \Big/\Big(6J((\gamma_e-\gamma_H)B_0,\tau_c) + 3J(\gamma_H B_0,\tau_c)\\ &\qquad + J((\gamma_e+\gamma_H)B_0,\tau_c)\Big)\\ &\approx \frac{5J(\gamma_e B_0,\tau_c)}{7J(\gamma_e B_0,\tau_c) + 3J(\gamma_H B_0,\tau_c)}, \qquad (10)\end{aligned}$$

where the final approximate form of Eq. (10) is derived from the approximations above and is the same as that given by Bennati *et. al.* for dipolar relaxation,[11] and where Eq. (9) comes from the definition[5,7] of ξ.

Alternatively, from Eqs. (7) and (8) we can then derive an expression for k_{low}, which we define to be

$$k_{low} \equiv \frac{5}{3}k_\rho - \frac{7}{3}k_\sigma \qquad (11)$$

From Eqs. (7), (8) and (11),

$$k_{low} \approx 5J(\gamma_H B_0,\tau_c), \qquad (12)$$

where again the approximation is nearly exact. We also note that k_{low} is of comparable magnitude to k_σ, and from Eqs. (9) and (11).

$$\xi(B_0,\tau_c) = \left(\frac{7}{5} + \frac{3}{5}\frac{k_{low}}{k_\sigma}\right)^{-1} \qquad (13)$$

References

(1) Kiselev, M.; Lesieur, P.; Kisselev, A.; Grabielle-Madelmond, C.; Ollivon, M. *J. Alloys Compd.* **1999**, *286*, 195–202.
(2) Cheng, C.-Y. Personal Communication.
(3) Hofmann, G. *ISCOTABLES : a handbook of data for biological and physical scientists*; Instrumentation Specialties Company: Lincoln, Neb., 1977.
(4) Armstrong, B. D.; Lingwood, M. D.; McCarney, E. R.; Brown, E. R.; Blümler, P.; Han, S. *J. Magn. Reson.* **2008**, *191*, 273–81.
(5) Franck, J. M.; Pavlova, A.; Han, S. *arxiv:1206.0510* **2012**, 25.
(6) Armstrong, B. D.; Han, S. *J. Chem. Phys.* **2007**, *127*, 104508.
(7) Hausser, K. H.; Stehlik, D. *Adv. Magn. Reson.* **1968**, *3*, 79–139.
(8) Armstrong, B. D.; Han, S. *J. Am. Chem. Soc.* **2009**, *131*, 4641–7.
(9) Türke, M.-T.; Bennati, M. *Phys. Chem. Chem. Phys.* **2011**, *13*, 3630–3.
(10) Hwang, L.; Freed, J. *J. Chem. Phys.* **1975**, *63*, 4017.
(11) Bennati, M.; Luchinat, C.; Parigi, G.; Türke, M.-T. *Phys. Chem. Chem. Phys.* **2010**, *12*, 5902–10.

[3] Note that for simplicity, we are either approximating or lumping chemical shift and g factor terms into the γ; the same math holds if we were to explicitly include these.